THE JOURNAL OF PHYSICAL CHEMISTRY B

Article

pubs.acs.org/JPCB

Structural, Dynamic, and Transport Properties of Concentrated Aqueous Sodium Chloride Solutions under an External Static Electric Field

Gan Ren, Rui Shi, and Yanting Wang*

State Key Laboratory of Theoretical Physics, Institute of Theoretical Physics, Chinese Academy of Sciences, 55 East Zhongguancun Road, P.O. Box 2735, Beijing, 100190 China

ABSTRACT: In the absence of an external electric field, it has already been known that ion clusters are formed instantaneously in moderately concentrated ionic solutions. In this work, we use molecular dynamics (MD) simulations to investigate the changes of structural, dynamic, and transport properties in a sodium chloride solution under an external electric field from the ion cluster perspective. Our MD simulation results indicate that, with a strong external electric field E ($\geq$0.1 V/nm) applied, ion clusters become smaller and less net charged, and the structures and dynamics as well as transport properties of the ion solution become anisotropic. The influence of the cluster structure and shell structure to transport properties was analyzed and the Einstein relation was found invalid in this system.

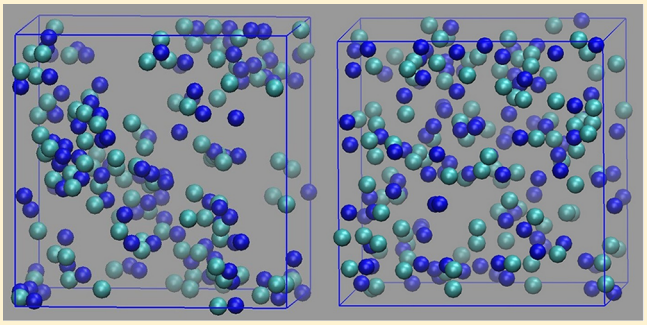

1. INTRODUCTION

Ionic solutions play an essential role in many scientific and engineering areas, such as chemical engineering[1−4] and biology.[5−7] After the proposition of the Debye−Hückel theory[8] describing the infinitely dilute strong electrolyte solutions, the thermodynamic and transport properties of dilute solutions have been extensively investigated.[9,10] Moreover, some extended theories were also applied to dilute weak electrolyte solutions.[9] In contrast, ions are likely to associate to form clusters in concentrated solutions,[11] for which the Debye−Hückel approximation is not applicable, and thus it is very difficult to predict solution behavior.

The formation of ion cluster (a set of ions spatially close to each other) in ionic solutions was proposed a long time ago based on the analysis of the discrepancies between theoretical and experimental results.[9] Recently, some experiments[12−16] have directly or indirectly detected the ion cluster formation at ambient conditions. Many simulations have also observed the cluster formation in sodium chloride (NaCl) solutions under ambient conditions[17−20] and supercritical conditions.[21,22] The nucleation mechanism[23,24] of ions in saturated solutions, nucleation at interface,[25] and the cluster morphology in NaCl solutions[26,27] were exploited by simulation. Theoretically, Scatchard's empirical model[28,29] can provide good thermodynamic properties comparable with experiments for concentrated solutions. Pitzer's semiempirical model[30−32] can be applied to electrolyte solutions as concentrated as 6 M. However, both models suffer from the same theoretical problem that they are nonlinear and do not satisfy the superposition principle for electric fields.[33]

After the proposition of the Debye−Hückel theory, many theories have been developed to investigate the transport properties of ionic solutions. Two main categories of mobility theories are continuum models of mobility[34−39] and molecular theories.[40] The continuum models separate the system friction into the hydrodynamic friction which is the usual Stokes friction in hydrodynamics, and the dielectric friction which is the central focus of developing the continuum models. The molecular theories calculate the dielectric friction by using the random force correlation function in the Brownian limit which is separated into a hard repulsive term and a soft attractive term. Moreover, Onsager's limiting conductivity theory[41] is able to describe the conductivity of diluted ionic solutions but not concentrated ionic solutions due to strong ion association. In the linear response regime close to equilibrium, certain theories have been developed to describe the relations between mobility, diffusion, and conductivity. In particular, mobility and diffusion are connected by the Einstein relation.[9]

Mobility and diffusion of ionic solutions have also been investigated by computer simulation. Lee and Rasaiah[42] simulated the case of an extremely dilute solution containing only one ion driven by an external electric field and found that the external field changes the drift velocity and mean square displacement, but not the shell structure and velocity correlation function. Extremely dilute solutions with real and virtual ions as well as neutral atoms were also simulated to explore the effect of solvation structure on particle mobility.[43] The friction

Received: December 3, 2013
Revised: March 21, 2014
Published: April 1, 2014

dx.doi.org/10.1021/jp4118387 | J. Phys. Chem. B 2014, 118, 4404−4411

coefficients of ions in solution at the ambient condition were also investigated[44] and the charge transport and ion−ion correlation in ionic liquids were found to be different from electrolyte solutions.[45] In addition, Murad[46] simulated a concentrated ionic solution under different external electric fields and discovered the relaxation effect of an electric field on the solvation shell, the activation process of ion movement, and the nonlinear response of ion dynamics. Yang et al.[47] investigated ionic solutions at different concentrations under an alternating electromagnetic field by both experiment and simulation, and found that the diffusion and ion mobility decrease with increasing concentration and increasing temperature. Despite the above investigations on ionic solutions, it is still unclear how ion clusters and shell structures change with an external electric field.

In this work, we choose the aqueous sodium chloride solution with a concentration of 2 M as an example of concentrated ionic solutions and use molecular dynamics (MD) simulations to systematically investigate the influence of an external static electric field on the structural, dynamic, and transport properties of concentrated ionic solutions. Our MD simulation results indicate that, with a strong external electric field E applied, ion clusters become smaller and have less net charges, the structures and dynamics as well as transport properties of the ionic solution become anisotropic, and the change of ion clusters and microscopic shell structures with the external field significantly influences the ion transport properties. The Einstein relation was also found to break down for driven ionic solutions, similar to the case of ionic liquids.[48]

2. SIMULATION METHODS

In order to roughly estimate the saturation point of NaCl at the temperature T = 300 K and the pressure P = 1 atm, we did the MD simulations at several concentrations for aqueous NaCl solutions with the AMBER 94 force field[49,50] and TIP3P water models.[51] The radial distribution functions (RDFs) calculated based on the simulation data are shown in Figure 1. It can be seen

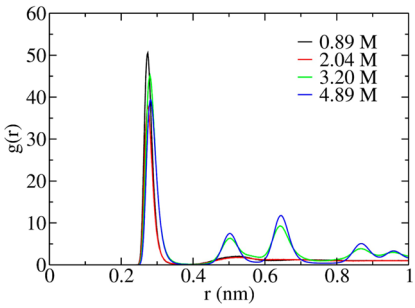

Figure 1. Na−Cl radial distribution functions at T = 300 K and P = 1 atm.

that the RDFs at the concentrations of 0.89 and 2.04 M, respectively, have a high first peak and a wavy tail with small fluctuations, which exhibits the feature of a liquid state. In contrast, the RDFs at 3.20 and 4.89 M have several separated high peaks, showing the feature of a solid state. Therefore, we estimate that the saturation point of the NaCl solution with the AMBER 94 and TIP3P force fields is well above 2.04 M and below 3.2 M. We want to emphasize that this estimation does not mean to accurately allocate the exact saturation point, as the serious work done by Moucka et al.,[52] but to roughly know the range of the saturation point to facilitate our choice of a suitable concentration for our simulations below.

Moreover, Hassan[27] showed that, when the concentration is above 1 M, clusters with more than ten ions form in the NaCl solution after the simulations were conducted for about 10−20 ns. On the basis of those factors, we chose to simulate the NaCl solution at the concentration of 2 M, which is below the saturation concentration and at the same time apparent ion cluster formation takes place. Six different electric fields E = 0, 0.1, 0.25, 0.5, 0.75, and 1 V/nm were applied to the X direction of the simulated system, respectively. All our MD simulations were carried out with the GROMACS package[53,54] and the system temperature was kept constant by the Nosé−Hoover thermostat.[55,56] In the simulation software, the external electric field took effect on a charged atom i (with a partial charge q_i and a mass m_i) by applying an additional electric force $q_i\vec{E}$ besides the usual MD forces in equilibrium $\vec{F}_i^{\mathrm{MD}}$. Correspondingly, the equation of motion is $m_i(d^2\vec{r}_i)/(dt^2) = \vec{F}_i^{\mathrm{MD}} + q_i\vec{E}$, where $\vec{r}_i$ is the position of atom i and t is the time. The simulated system contains 2700 water molecules, 105 sodium ions, and 105 chloride ions in a periodic cubic box with a side length of 4.40 nm, corresponding to a concentration of about 2 M. The periodic boundary conditions were applied to all three dimensions and the particle-mesh Ewald algorithm[57,58] was employed to calculate the long-range electrostatic interactions. The time step for all MD simulations was 1 fs. For each E, a constant NPT MD simulation was first performed at T = 300 K and P = 1 atm for 2 ns to determine the system density, followed by a 4 ns constant NVT MD simulation at T = 300 K to allow the system to reach its nonequilibrium steady state. To improve statistics, the NVT procedure was independently repeated 20 times with their initial configurations randomly sampled from a constant NVT MD simulation at T = 2000 K, whose density was fixed to 1.07 g/cm^3 determined at T = 300 K. For each of the 20 simulations, the simulation time was 2 ns and 2000 instantaneous configurations were sampled every 1000 steps for data analysis.

3. RESULTS

3.1. Ion clusters. As described in the Introduction, it has been known that instantaneous ion clusters usually form in concentrated ionic solutions. To quantitatively study ion clusters in solution, we adopted the definition of ion clusters given in ref 27, namely, an ion cluster is defined as an array of ions with each ion connected with at least one other ion. Two ions are considered connected when their distance is within a certain cutoff, which was selected in this work as 3.8 Å, the position of the first valley of the Na−Cl RDF. Through this paper, we denote either an individual ion or an ion cluster as a particle.

The numbers of ions forming different sizes of particles are shown in Figure 2a. With an increasing external electric field, ions with opposite charges experience larger forces in opposite directions, which segregate large clusters into smaller ones. On the other hand, increasing E allows more single ions to aggregate and form small clusters to reduce the total net charge of particles. The competition between these two factors results in the decrease of the number of single ions and the increase of the number of clusters containing 2−10 ions with E, as shown in Figure 2a. Although as shown in Figure 2b, the decreased numbers of single ions and large clusters with E results in the increase of both the total number of clusters and the overall net charges, the average net charges taken by positive and negative particles, respectively, decrease with E, as shown in Figure 2c. This phenomenon can be qualitatively understood by the following argument. In the absence of the external electric field, the ion cluster distribution in the solution is determined by the

dx.doi.org/10.1021/jp4118387 | J. Phys. Chem. B 2014, 118, 4404−4411

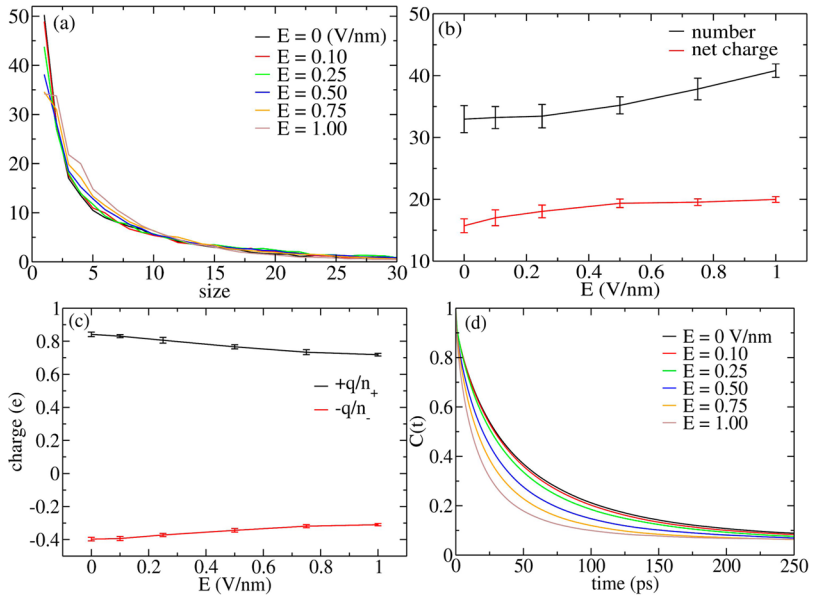

Figure 2. (a) Number of ions forming particles with different sizes. (b) Number of clusters and net charges they take. (c) Ratio of net charges of positive or negative particles with respect to their numbers. (d) Time correlation functions of clusters quantifying their lifetimes.

competition between the molecular interactions and the thermal energy. When an E is applied, the oppositely net-charged ion clusters feel effective Coulomb forces in opposite directions. Therefore, the system responds to the increase of the external electric field by decreasing the average charge each ion takes, so that the effective forces felt by ions are reduced and the new balance contrast to the thermal energy is reached with a different ion cluster distribution. Moreover, more clusters are positively charged, probably due to the anisotropy of the aqueous solvation environment formed by water molecules, whose negative charge density is higher than positive charge density.

The time correlation function quantifying the mean lifetime of a cluster[42] is defined as

$$C(t) = \frac{1}{A}\sum_{i=2}^{N}\sum_{t_0}^{T_s/2}\vartheta_i(t_0)\vartheta_i(t_0 + t) \quad (1)$$

where A is a normalization constant, ϑ is a delta function whose value is 1 if a cluster with i ions still exists at time t and zero otherwise, N is the size of the largest cluster, and T_s is the sample time. As shown in Figure 2d, when E is larger than 0.25 V/nm, the cluster lifetime significantly decreases with increasing E, consistent with the description given by Onsager's theory,[59] which shows that a dilute weak electrolyte solution under an electric field deviates from Ohm's law by increasing its dissociation constant and accelerating the dissociation process. Since ions associate to form clusters in a concentrated NaCl solution, it can also be regarded effectively as a weak electrolyte solution and thus Onsager's theory can be applied to explain the decrease of its lifetime with E in this system.

3.2. Shell Structures and Dynamics. We then calculated the Na−Cl, Na−water, and Cl−water RDFs around a central ion to examine the effect of the external electric field on the local structures of the system. As an external electric field is applied, the local structures should become different for the two directions parallel and perpendicular to the field direction. In addition, the local structures along and opposite to the field direction should also be different. Therefore, the angle-resolved RDFs (ARRDFs)[48] were employed to quantify the spatial asymmetry of the structure. An ARRDF is defined as the RDF falling into the cone region with an angle cutoff θ_c around the X, Y, or Z axes, which is just the regular RDF not averaged in all directions but in a solid angle. The ARRDF can be expressed as $g(r) = \langle\delta(r - r_1)\rangle$, where δ takes 1 when the azimuth of vector $r - r_1$ with respect to the designated direction is smaller than θ_c or larger than $\pi - \theta_c$, and takes zero otherwise. In this work, we choose $\theta_c = \pi/6$ and the positive direction (the azimuth smaller than θ_c) and the negative direction (the azimuth larger than $\pi - \theta_c$) were calculated separately.

With an external E applied, the ion atmosphere should also become asymmetric, which can be quantified by the angle distribution function (ADF) defined as

$$g(\theta) = \frac{1}{A}\sum_{i\neq j}^{N}\vartheta(|\vec{r_i} - \vec{r_j}|, \phi, \theta) \quad (2)$$

where r_i is the position vector of the ith ion, φ is the zenith angle and θ is the azimuth angle, $\vartheta(|\vec{r}|,\varphi,\theta)$ is the Heaviside unit step function taking 1 if $|\vec{r}| < r_c$ and $-\varphi_c < \phi < \varphi_c$ and 0 otherwise, A is the normalization factor, and N is the total number of ions in this region. As illustrated in the inset in Figure 4a, the ADF actually counts the average number of ion pairs inside the spherical region with a radius of r_c excluding the two cones. In this work, we choose r_c = 3.8 Å and $\varphi_c = \pi/3$.

The ARRDFs of Na−Cl (Cl^- is at the center) at different electric fields are shown in Figure 3 and the ADFs are shown in Figure 4. It is obvious that under an external electric field, the solution structure is not isotropic anymore. Because of symmetry, the Y and Z directions, which are perpendicular to the X direction along which E is applied, are always identical, so only the results in the X and Y directions are plotted. The first peaks in the Na−Cl ARRDFs correspond to the ion atmosphere defined in the Debye−Hückel theory, and the high peaks indicate that the ions are strongly associated in the solution, consistent with the cluster formation data shown in Figure 2. In the absence of E, the ARRDFs in all directions are identical. When an E is applied, the first-peak height and width of the X+ ARRDFs significantly increase with E, but the X− and Y+ ARRDFs have

dx.doi.org/10.1021/jp4118387 | J. Phys. Chem. B 2014, 118, 4404−4411

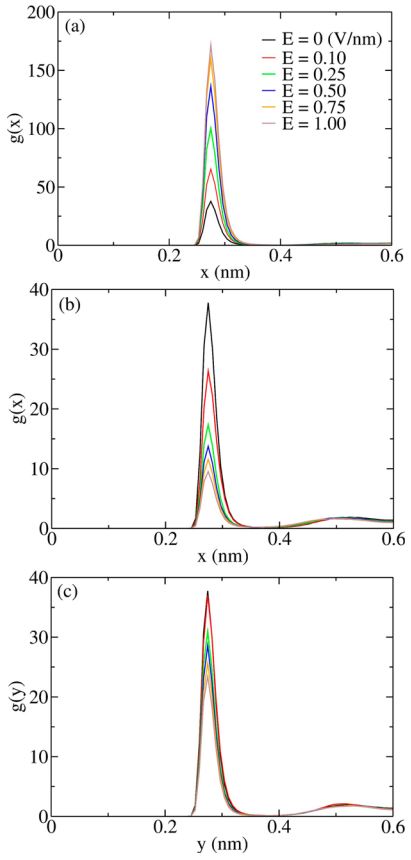

Figure 3. Na−Cl ARRDFs under different external electric fields in the $X+$ direction (a), the $X-$ direction (b), and the $Y+$ direction (c).

the opposite trend, indicating that more counterions distribute in the $X+$ direction than in the $X-$ direction and Y direction. Consistently, the ADF data shown in Figure 4 indicate that, with an increasing E, more ions distribute in the $X+$ direction and less in the $X-$ direction, and less ions are in the directions perpendicular to E although they always distribute uniformly in those directions. This ion rearrangement effectively balances the applied external electric field.

The ARRDFs of water shells are shown in Figure 5. The ion−water ARRDFs (ion is at the center) have much lower first peaks than the Na−Cl ARRDFs, and the trends of the first-peak height and width changes are opposite, because more ions occupy the positions along the $X+$ direction and water molecules are forced to distribute more along other directions. In contrast, the Cl−water ARRDFs show almost the same trend as the Na−Cl ARRDFs because sodium and chloride ions take opposite charges and the space they occupy is correlated. Moreover, the Na−water and Cl−water ARRDFs show a distinctive feature that the external electric field only evidently affects the first hydration shell of Na^+, but the influence extends to the second and third hydration shells of Cl^-, which may be attributed to the anisotropy of water orientations around Na^+ and Cl^-[29] that the oxygen atom of a water molecule is more likely to orient toward Na^+ and the two hydrogen atoms tend to orient toward Cl^-. This anisotropy of water molecules leads to different structural changes of the Na^+ and Cl^- hydration shells under an external electric field.

The dynamics of ion atmospheres and hydration shells characterized by the residence correlation functions[42] are shown in Figure 6. The lifetime of each shell decreases with increasing E because the stronger opposite forces applied on counterions make ions more likely to be apart and thus the deformed shell structure becomes less stable, consistent with the data shown in Figure 2. Since the interactions between two ions are stronger than those between one ion and one water molecule, the lifetimes of ion atmospheres are much longer than hydration shells. Besides the structural change described above, the anisotropy of water molecules is also responsible for the slightly longer Na^+ hydration shell lifetime than Cl^-.

3.3. Drift Velocity and Mobility. The ion drift velocity and mobility are two important quantities characterizing the transport properties of an ionic solution. When an external electric field is applied, the displacement of an ion $X(t)$ consists of two parts: random diffusive displacement $X_r(t)$ due to thermal motion and unidirectional drift displacement $v_d t$ driven by E:

$$X(t) = X_r(t) + v_d t \tag{3}$$

where v_d is drift velocity and t is time. Taking the ensemble-average of both sides and considering the randomness condition

$$\lim_{t\to\infty} \langle X_r(t)\rangle = 0 \tag{4}$$

One obtains

$$v_d = \lim_{t\to\infty} \frac{\langle X(t)\rangle}{t} \tag{5}$$

In our MD simulations, we performed 20 independent trajectories to accurately determine the drift velocity, as had been done for ionic liquid systems.[48] The mobility u is defined as

$$u = \frac{v_d}{E} \tag{6}$$

The drift velocities and mobilities of ions and water molecules are shown in Figure 7, parts a and b. The drift velocities of ions and all water molecules increase nonlinearly when E ranges from 0.10 to 1.0 V/nm. The drift velocities of water molecules result

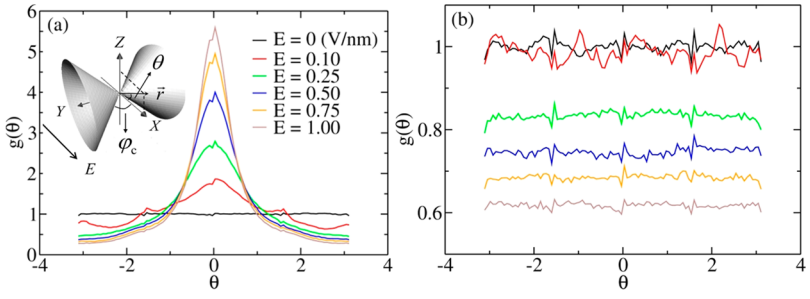

Figure 4. Na−Cl ADFs under different external electric fields in the XZ plane (a) and the YZ plane (b). The inset in part a is the schematic of the angle distribution function.

dx.doi.org/10.1021/jp4118387 | J. Phys. Chem. B 2014, 118, 4404−4411

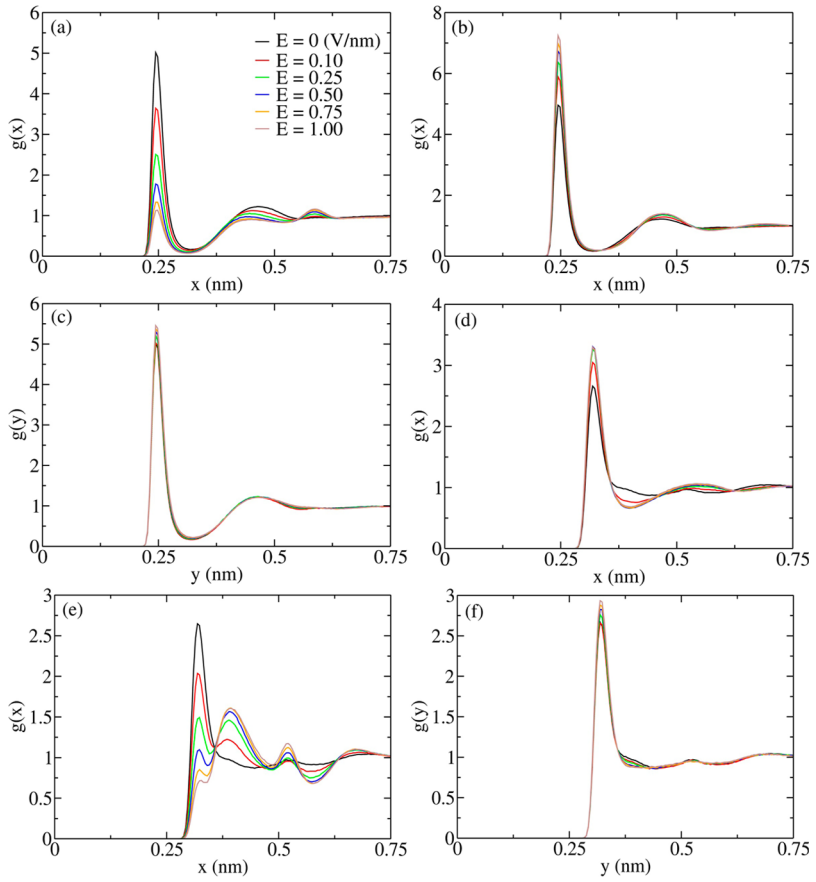

Figure 5. ARRDFs of water shells under different external electric fields. (a) Na^+ water shell in the *X*+ direction. (b) Na^+ water shell in the *X*- direction. (c) Na^+ water shell in the *Y*+ direction. (d) Cl^- water shell in the *X*+ direction. (b) Cl^- water shell in the *X*− direction. (c) Cl^- water shell in the *Y*+ direction.

from dragging by the solvated ions. As shown in Figure 7c, the mobilities of both cations and anions are not constants, but first decrease and then increase, and their values are much larger than those reported for weak electric fields.[9,10] The increase of ion mobility with the external electric field was previously reported by Wien,[9] and a microscopic mechanism proposed by Onsager and Kim[61] attributes the increase of mobility to the separation of the central ion and its nearest counterions, which can also be applied to explaining our results.

In a steady state, the effective friction force on an ion by the ion atmosphere $f_r = \alpha v_d$ is equal to the electric force on the ion $F_e = qE$, where α is the frictional constant and q is the ion charge. Thus, we obtain

$$u = \frac{v_d}{E} = \frac{q}{\alpha} \tag{7}$$

If we assume the Stokes law is satisfied in our system, we obtain

$$\alpha \propto R_H \Rightarrow u \propto \frac{q}{R_H} \tag{8}$$

where R_H is the hydrodynamic radius, whose value for an ion cluster can be calculated by the Bloomfield equation[60]

$$R_H^k = (\sum_{i=1}^{n} \rho_i^2)^2 [\sum_{i=1}^{n} \rho_i^3 + \sum_{i=1}^{n} \sum_{j \neq i}^{n} \rho_i^2 \rho_j^2 \langle r_{ij}^{-1} \rangle_k]^{-1} \tag{9}$$

and for a single ion by

$$R_H^k = \rho_k \tag{10}$$

where ρ_i is the hydrodynamic radius of a single ion ($\rho(Na^+)$ = 0.1980 nm and $\rho(Cl^-)$ = 0.1691 nm in our system, determined by the method reported in ref 26), r_{ij} is the distance between ion i and ion j in a cluster, $\langle\ \rangle_k$ denotes the average over all clusters with size k in one sampled configuration, and R_H^k is the hydrodynamic radius of cluster k. With these relations, eq 6 for cation and anion can be expressed as

$$\Delta u^{\pm} \propto \sum_k \frac{q_k^{\pm}}{R_H^{k\pm}} \tag{11}$$

where $\Delta u^{\pm}$ is the mobility and $q_k^{\pm}$ and $R_H^{k\pm}$ are the charge and hydrodynamic radius for cluster k, respectively. The related results are shown in Figure 7d, which exhibit almost the same trend as the mobility shown in Figure 7c. Therefore, the nonmonotonical change of ion mobility with increasing E results from the competition between the tendency of lowering the net charges of ion clusters and the decrease of the hydrodynamic radius.

3.4. Self-Diffusion. Another important transport property of ionic solutions is the self-diffusion driven by thermal energy. For a nonequilibrium steady state, the drift velocity caused by the external field has to be deducted from the total velocity to obtain the self-diffusion coefficient, so the Einstein equation in the X direction becomes

$$\lim_{t \to \infty} \langle X(t) - v_d t \rangle^2 = 2D_X t \tag{12}$$

dx.doi.org/10.1021/jp4118387 | J. Phys. Chem. B 2014, 118, 4404−4411

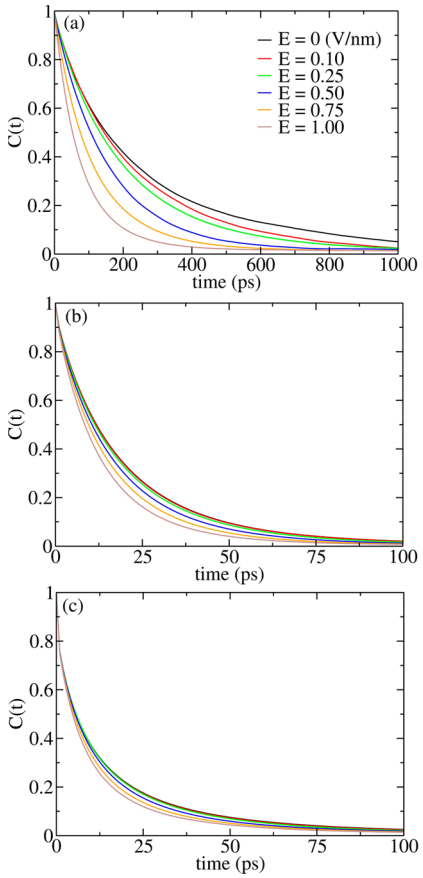

Figure 6. Residence correlation functions of the ion atmosphere (a), Na^+ hydration shell (b), and Cl^- hydration shell (c) under different electric fields.

where D_X is the effective self-diffusion coefficient in the X direction. The mean square displacements (MSDs) for various components in different directions are shown in Figure 8 and the corresponding self-diffusion coefficients are shown in Figure 9. The MSDs are all proportional to time, which indicates that the modified Einstein equation in eq 12 is still valid. The diffusion coefficients of ions increase with E in all directions, in agreement with Yang and Huang's work,[47] which can be understood by considering that the clusters become smaller and less charged, as shown in Figure 2. The diffusion coefficients in the X direction are much larger than in the Y direction when E is applied, because the ion atmosphere or the water shell is anisotropically distorted, resembling the ion cage distortion in ionic liquids.[48] In addition, Cl^- diffuses faster than Na^+ due to the asymmetric nature of water molecules.

For simple liquids in the linear-response region, the diffusion coefficient and the mobility satisfy the Einstein relation

$$D = uk_BT \tag{13}$$

where k_B is the Boltzmann constant and T is temperature. As shown in Figures 7c and 9, for our studied system, D and u show different responses to the external electric field: the former increases with E but the latter slightly decreases and then slightly increases, indicating that the Einstein relation is invalid for our studied system driven by a strong E which is out of the linear-response regime. Recently, a microscopic mechanism attributes the deviation of the Einstein relation in the KSCN solution to ion association.[62] The Einstein relation was also found breakdown for ionic liquids under a strong external electric field.[48]

4. CONCLUSIONS

In conclusion, we have carried out a series of MD simulations for a concentrated NaCl solution under different external electric fields. In a concentrated solution, ions associate to form clusters. We studied the changes of cluster sizes and net charges with respect to the external electric field E and found that clusters become smaller and less charged with increasing E. Moreover, the local structures as well as the dynamic and transport properties become anisotropic under a strong electric field, consistent with the results for ionic liquids.[48] The ARRDFs indicate that, with an E applied, the first-shell structure around an ion or a water molecule is distorted from spherical to ellipsoid, and ions in an ion atmosphere distribute more along the field direction but water molecules in a hydration shell distribute less

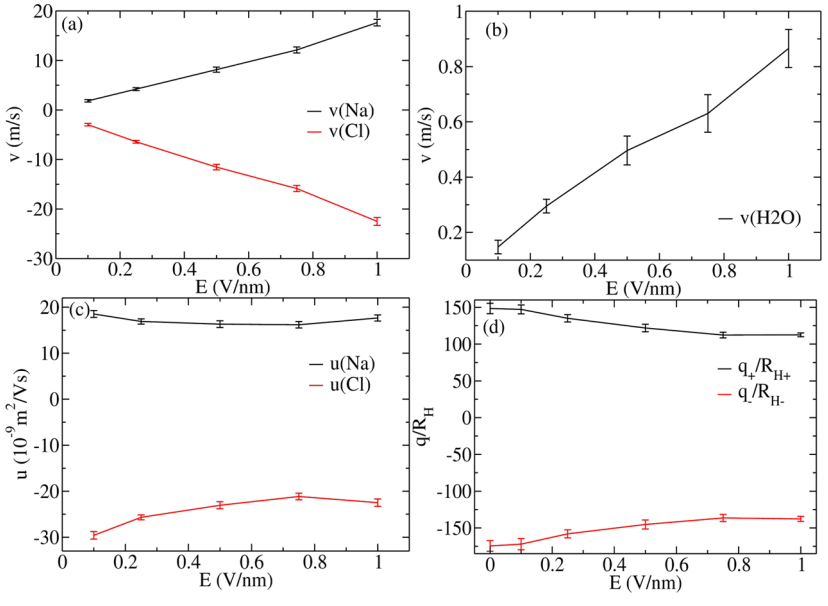

Figure 7. (a) Drift velocities of ions. (b) Drift velocities of water molecules. (c) Ion mobility. (d) Charges divided by the hydrodynamic radii.

dx.doi.org/10.1021/jp4118387 | J. Phys. Chem. B 2014, 118, 4404−4411

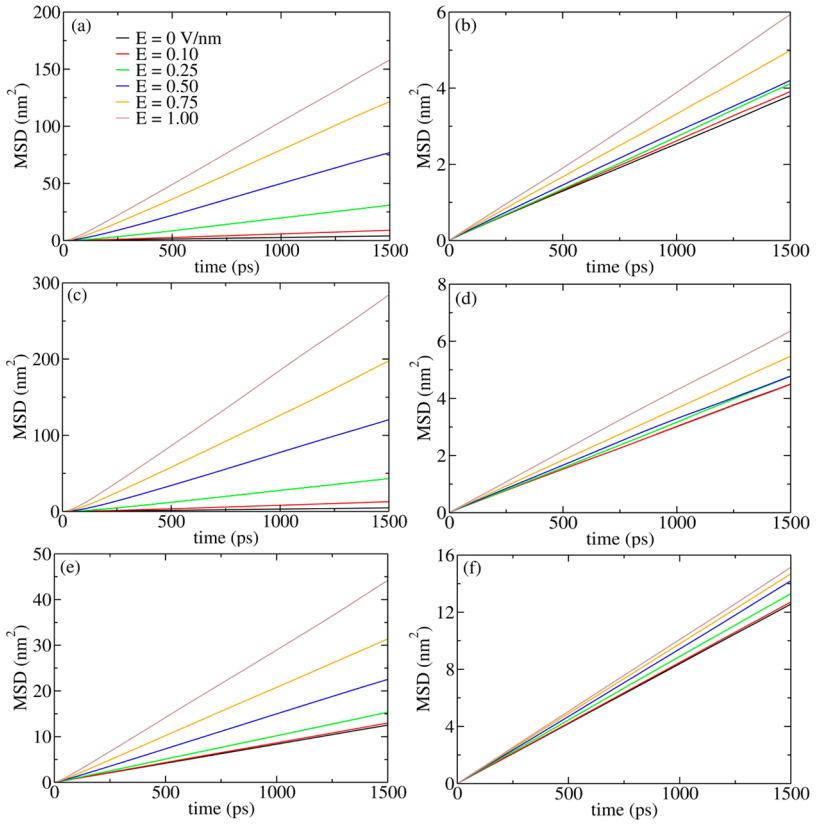

Figure 8. MSDs as a function of E for Na^+ (first row), Cl^- (second row), and water molecules (third row). The left column shows the MSDs in the X direction and the right column shows the MSDs in the Y direction.

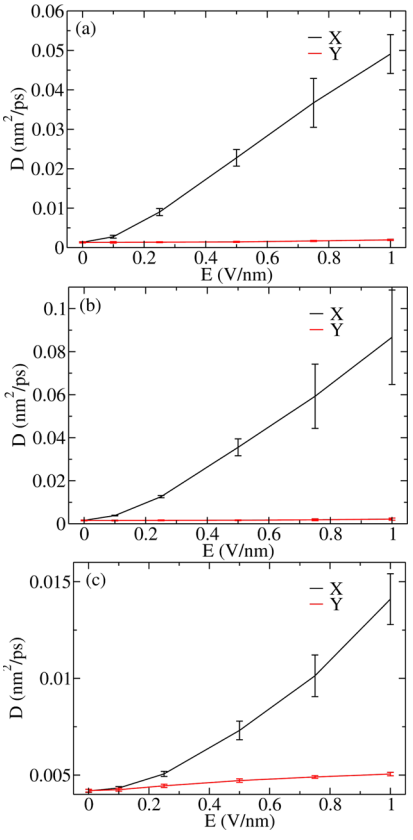

Figure 9. Diffusion coefficients as a function of the external electric field for Na^+ (a), Cl^- (b), and water molecules (c), respectively.

along the field direction. The analysis of the transport properties demonstrates that the drift velocities of all components increase with E, and the mobilities of ions slightly decrease and then slightly increase with E. Diffusion coefficients increase with E in all directions but much faster along the field direction, and the shell dynamics decrease with E. We also found that the different solvation structures of Na^+ and Cl^- result in different response, the velocity increase of Cl^- is larger than Na^+, and the mobility and diffusion of Cl^- are larger than Na^+. The Einstein relation is invalid in this system due to the complex ion-cluster structure as well as the far-from-equilibrium condition under a strong external field. The phenomena we have observed and the mechanisms we have proposed are anticipated to be helpful for the applications of ionic solutions in nonequilibrium states, such as plating, electrophoresis, and battery.

On the other hand, the cluster formation in ionic solutions may play an important role in ion nucleation and crystallization in ionic solutions.[63] Since ionic solutions frequently work under an external electric field, it is of interest to understand the influence of the external electric field to the ion nucleation and crystallization process. In particular, it is interesting to see how the saturation concentration changes with the electric field. Our present work demonstrates that the average size of ion clusters tends to be smaller with increasing field strength, because the stronger electric field makes ions more difficult to associate, therefore it is natural to postulate that the saturation concentration may increase with the field strength. As the field strength increases, more clusters might be segregated, and it seems reasonable that eventually there might exist a critical field strength when any concentration of ions cannot crystallize. Under such a strong electric field, the static definition of ion

dx.doi.org/10.1021/jp4118387 | J. Phys. Chem. B 2014, 118, 4404−4411

clusters might not work well and a dynamic definition introduced by Hassan's work[27] may be necessary. More simulations and analyses are required to study this interesting problem.

AUTHOR INFORMATION

Corresponding Author

*(Y.W.) E-mail: wangyt@itp.ac.cn. Telephone: +86 10-62648749.

Notes

The authors declare no competing financial interest.

ACKNOWLEDGMENTS

This work was supported by the National Basic Research Program of China (973 Program, No. 2013CB932804), the National Natural Science Foundation of China (Nos. 91227115 and 11121403) and the Hundred Talent Program of the Chinese Academy of Sciences (CAS). The authors thank the Supercomputing Center in the Computer Network Information Center at the CAS for allocations of computer time.

REFERENCES

(1) Equey, J.-F.; Müller, S.; Tsukada, A.; Haas, O. *J. Appl. Electrochem.* **1989**, *19*, 65−68.
(2) Yoshida, H.; Sone, M.; Mizushima, A.; Abe, K.; Tao, X. T.; Ichihara, S.; Miyata, S. *Chem. Lett.* **2002**, *31*, 1086−1087.
(3) Conway, B. *Chem. Soc. Rev.* **1992**, *21*, 253−261.
(4) Zare, R. N. *Science* **1988**, *242*, 224−228.
(5) Gurau, M. C.; Lim, S.-M.; Castellana, E. T.; Albertorio, F.; Kataoka, S.; Cremer, P. S. *J. Am. Chem. Soc.* **2004**, *126*, 10522−10523.
(6) Zhang, Y.; Cremer, P. S. *Curr. Opin. Chem. Biol.* **2006**, *10*, 658−663.
(7) Roux, B.; Karplus, M. *Annu. Rev. Biophys. Biomol. Struct.* **1994**, *23*, 731−761.
(8) Debye, P.; Hückel, E. *Phys. Z.* **1923**, *24*, 185−206.
(9) Robinson, R. A.; Stokes, R. H. *Electrolyte Solutions*; Dover Publications: New York, 2002.
(10) Harned, H.; Owen, B. *The physical chemistry of electrolytic solutions*; Reinhold Publishing: New York, 1958.
(11) Marcus, Y.; Hefter, G. *Chem. Rev.* **2006**, *106*, 4585−4621.
(12) Georgalis, Y.; Kierzek, A. M.; Saenger, W. *J. Phys. Chem. B* **2000**, *104*, 3405−3406.
(13) Rusli, I.; Schrader, G.; Larson, M. *J. Cryst. Growth* **1989**, *97*, 345−351.
(14) Cerreta, M. K.; Berglund, K. A. *J. Cryst. Growth* **1987**, *84*, 577−588.
(15) Bian, H.; Wen, X.; Li, J.; Chen, H.; Han, S.; Sun, X.; Song, J.; Zhuang, W.; Zheng, J. *Proc. Natl. Acad. Sci. U.S.A.* **2011**, *108*, 4737−4742.
(16) Pouget, E. M.; Bomans, P. H.; Goos, J. A.; Frederik, P. M.; Sommerdijk, N. A. *Science* **2009**, *323*, 1455−1458.
(17) Chialvo, A. A.; Simonson, J. M. *J. Mol. Liq.* **2007**, *134*, 15−22.
(18) Smith, D. E.; Dang, L. X. *J. Chem. Phys.* **1994**, *100*, 3757−3766.
(19) Fennell, C. J.; Bizjak, A.; Vlachy, V.; Dill, K. A. *J. Phys. Chem. B* **2009**, *113*, 6782−6791.
(20) Degrève, L.; da Silva, F. L. B. *J. Chem. Phys.* **1999**, *110*, 3070−3078.
(21) Chialvo, A.; Cummings, P.; Cochran, H.; Simonson, J.; Mesmer, R. *J. Chem. Phys.* **1995**, *103*, 9379−9387.
(22) Sherman, D. M.; Collings, M. D. *Geochem. Trans.* **2002**, *3*, 102−107.
(23) Zahn, D. *Phys. Rev. Lett.* **2004**, *92*, 040801.
(24) Alejandre, J.; Hansen, J.-P. *Phys. Rev. E* **2007**, *76*, 061505.
(25) Yang, Y.; Meng, S. *J. Chem. Phys.* **2007**, *126*, 044708.
(26) Hassan, S. A. *Phys. Rev. E* **2008**, *77*, 031501.
(27) Hassan, S. A. *J. Phys. Chem. B* **2008**, *112*, 10573−10584.
(28) Scatchard, G. *J. Am. Chem. Soc.* **1961**, *83*, 2636−2642.
(29) Scatchard, G.; Rush, R. M.; Johnson, J. S., Jr. *J. Phys. Chem.* **1970**, *74*, 3786−3796.
(30) Pitzer, K. S. *J. Phys. Chem.* **1973**, *77*, 268−277.
(31) Pitzer, K. S.; Mayorga, G. *J. Phys. Chem.* **1973**, *77*, 2300−2308.
(32) Pitzer, K. S.; Mayorga, G. *J. Solution Chem.* **1974**, *3*, 539−546.
(33) Griffiths, D. J. *Introduction to electrodynamics*. Pearson Education: Dorling Kindersley: New York, 2007.
(34) Fuoss, R. M. *Proc. Natl. Acad. Sci. U.S.A.* **1959**, *45*, 807−813.
(35) Boyd, R. H. *J. Chem. Phys.* **1961**, *35*, 1281−1283.
(36) Zwanzig, R. *J. Chem. Phys.* **1963**, *38*, 1603−1605.
(37) Hubbard, J.; Onsager, L. *J. Chem. Phys.* **1977**, *67*, 4850−4857.
(38) Hubbard, J.; Kayser, R. *J. Chem. Phys.* **1981**, *74*, 3535−3545.
(39) Chen, J. H.; Adelman, S. *J. Chem. Phys.* **1980**, *72*, 2819−2831.
(40) Wolynes, P. G. *Annu. Rev. Phys. Chem.* **1980**, *31*, 345−376.
(41) Hemmer, P. C.; Holden, H.; Ratkje, S. K. *The collected works of Lars Onsager*; World Scientic: Singapore, 1996.
(42) Lee, S. H.; Rasaiah, J. C. *J. Chem. Phys.* **1994**, *101*, 6964−6974.
(43) Koneshan, S.; Rasaiah, J. C.; Lynden-Bell, R.; Lee, S. *J. Phys. Chem. B* **1998**, *102*, 4193−4204.
(44) Koneshan, S.; Lynden-Bell, R.; Rasaiah, J. C. *J. Am. Chem. Soc.* **1998**, *120*, 12041−12050.
(45) Kashyap, H. K.; Annapureddy, H. V.; Raineri, F. O.; Margulis, C. J. *J. Phys. Chem. B* **2011**, *115*, 13212−13221.
(46) Murad, S. *J. Chem. Phys.* **2011**, *134*, 114504.
(47) Yang, L.; Huang, K. *J. Phys. Chem. B* **2010**, *114*, 8449−8452.
(48) Shi, R.; Wang, Y. *J. Phys. Chem. B* **2013**, *117*, 5102−5112.
(49) Cornell, W. D.; Cieplak, P.; Bayly, C. I.; Gould, I. R.; Merz, K. M.; Ferguson, D. M.; Spellmeyer, D. C.; Fox, T.; Caldwell, J. W.; Kollman, P. A. *J. Am. Chem. Soc.* **1995**, *117*, 5179−5197.
(50) Sorin, E. J.; Pande, V. S. *Biophys. J.* **2005**, *88*, 2472−2493.
(51) Jorgensen, W. L.; Chandrasekhar, J.; Madura, J. D.; Impey, R. W.; Klein, M. L. *J. Chem. Phys.* **1983**, *79*, 926−936.
(52) Moucka, F.; Lísal, M.; Škvor, J. i.; Jirsák, J.; Nezbeda, I.; Smith, W. R. *J. Phys. Chem. B* **2011**, *115*, 7849−7861.
(53) Berendsen, H. J.; van der Spoel, D.; van Drunen, R. *Comput. Phys. Commun.* **1995**, *91*, 43−56.
(54) Van Der Spoel, D.; Lindahl, E.; Hess, B.; Groenhof, G.; Mark, A. E.; Berendsen, H. J. *J. Comput. Chem.* **2005**, *26*, 1701−1718.
(55) Nosé, S. *J. Chem. Phys.* **1984**, *81*, 511−519.
(56) Hoover, W. G. *Phys. Rev. A* **1985**, *31*, 1695−1697.
(57) Darden, T.; York, D.; Pedersen, L. *J. Chem. Phys.* **1993**, *98*, 10089−10092.
(58) Essmann, U.; Perera, L.; Berkowitz, M. L.; Darden, T.; Lee, H.; Pedersen, L. G. *J. Chem. Phys.* **1995**, *103*, 8577−8593.
(59) Onsager, L. *J. Chem. Phys.* **1934**, *2*, 599−615.
(60) Bloomfield, V.; Dalton, W.; Van Holde, K. *Biopolymers* **1967**, *5*, 135−148.
(61) Onsager, L.; Kim, S. K. *J. Phys. Chem.* **1957**, *61*, 198−215.
(62) Zhang, Q.; Xie, W.; Bian, H.; Gao, Y. Q.; Zheng, J.; Zhuang, W. *J. Phys. Chem. B* **2013**, *117*, 2992−3004.
(63) Hassan, S. A. *J. Chem. Phys.* **2011**, *134*, 114508.